Received: 6 September 2024 | *Revised:* 18 October 2024 | *Accepted:* 23 October 2024
DOI: 10.37917/ijeee.22.1.48 *Vol. 22 | Issue 1 | June 2026*

Iraqi Journal for Electrical and Electronic Engineering
Original Article

Open Access
IJEEE University of Basrah College of Engineering

Excitation Control Enhancement for the Synchronous Generator Using Effective Control Methodology

Hawraa N. Jasim*[1,2], Kasim K. Abdalla[2]
[1]Department of Electrical Engineering, Technical Institute of Babylon, Al-Furat Al-Awsat Technical University (ATU), Babylon, Iraq.
[2]Department of Electrical Engineering, Faculty of Engineering, University of Babylon, Babylon, Iraq.

Correspondance
*Hawraa N. Jasim
Department of Electrical Engineering, Technical Institute of Babylon,
Al-Furat Al-Awsat Technical University (ATU), Babylon, Iraq.
Email: hawraa.jasim.iba9@atu.edu.iq

Abstract
In electrical power plants, the excitation control system is an important part of controlling the output voltage of the synchronous generators. The purpose of this paper is to utilize various methods of excitation control, such as Proportional-Integral-Derivative (PID), Simulated Annealing (SA), and Neural Network (NN) controllers. Each method is examined in terms of its effectiveness in enhancing system stability, reliability, and adaptability to varying operational conditions. The study simulates and optimizes a 2 MVA/400 V synchronous generator driven by a three-phase diesel engine with mechanical coupling and an exciter system. MATLAB 2021 is used to implement the Simulink model. The dynamic responses of field voltage and field current to load changes were analyzed for each control technique. Additionally, the performance of three-phase voltage and current for synchronous generator were examined over a 10-second timeframe. Our findings indicate that the PID controller offers straightforward implementation and reliable performance under varying conditions. The NN controller implementation is more similar to the PID response, and the SA controller demonstrates superior adaptability. The research underscores the potential of integrating these advanced control techniques in synchronous generators, paving the way for enhanced stability and reliability in modern electric power systems, with further implications for renewable energy integration.

Keywords
Excitation control, Neural networks, Simulated annealing, Synchronous generator, mechanical coupling.

I. Introduction

The voltage control system acts as one of the main control systems in electric power plants [1]. The capacity of the engineer to supply the load with a reliable, continuous, and ideally optimally quality service is critical to the effective functioning of today's complex power systems. For the equipment that belongs to the end user to function properly, the load needs to be supplied at a steady frequency and voltage that are maintained within tight tolerances [2]. It is crucial to note that variations in the actual power output of electric generators mostly impact the voltage and frequency in the system. The above factors states that a generator has two main controllers. A governor regulates the generator's rotational speed or frequency, while an Automatic-Regulator of Voltage (AVR) keeps the generator's voltage at a set level. The AVR loop is made up of a lot of different devices/elements, including a synchronous, amplifier, exciter, controller, and many sensors. These are all combined into a single regulation contour along with other signals like the Power System Stabilizer (PSS) signal, VHz signal, generator current value, and excitation current value. Fig.1 shows the shared architecture of the AVR system, with e referring for the error signal, or the difference between the reference voltage V_{ref} and the terminal voltage V_t [3]. Even with the majority of electric power systems having AVR controller, these systems occasionally experience random vibrations at very low frequencies, often a

This is an open-access article under the terms of the Creative Commons Attribution License,
which permits use, distribution, and reproduction in any medium, provided the original work is properly cited.
©2026 The Authors.
Published by Iraqi Journal for Electrical and Electronic Engineering | College of Engineering, University of Basrah.

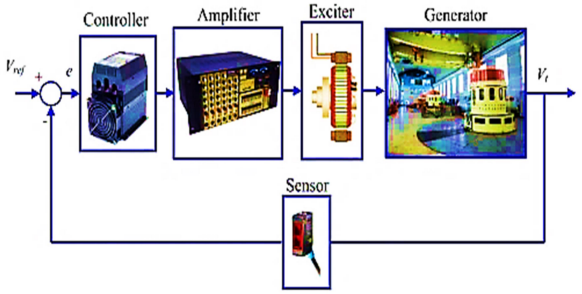

Fig. 1. The automatic voltage regulator system's general layout [3].

few cycles per minute. The oscillation at low frequencies is an undesirable phenomena. It is a part of the power systems. Large oscillations are another issue the system faces because of faults, temporary changes, and other disruptions. Small, slow changes in load applied to a generator in a power system result in a small signal (steady-state) stability issue. In the event that the three system variables (frequency, power, and voltage) do not return to their steady-state values within predetermined timeframes and levels after a little disruption, these variables will exhibit unstable or inadequately damped low frequency oscillations [4–6].

The estimation of regulator parameters involved the minimization of the related criterion function, also known as the objective function. The goal of the regulator was to attain the optimal response, that is, the desired generator voltage response, when the reference value altered from 0 to 1 Per Unit (p.u.) (nominal value). TableI shows the common objective functions that are used. ITAE stands for time multiplication by the error's absolute value [7], IAE for the error's integral value [8], ITSE for time multiplication by the error's weighted squared [9], and ISE for the error's squared integral [10]. The objective function ZLG is widely recognized and is named after the author who initially defined it, Zwe-Lee Gaing [3] The criteria function of the mix of ZLG and ITSE is shortened to OF [11].

Conventional excitation control techniques frequently fail to reduce oscillations because they are based on elementary algorithms. This paper uses various techniques of excitation control, such as employing a PID controller, a simulated annealing controller, and neural networks controller, to compare their effectiveness in achieving optimal stability and reliability in generator operation. The search's goal is to create a

TABLE I.
THE MOST POPULAR OBJECTIVE FUNCTIONS

NO.	common objective functions
1.	$ITAE = \int t\|e(t)\|dt$
2.	$IAE = \int \|e(t)\|dt$
3.	$ITSE = \int te^2(t)dt$
4.	$ISE = \int e^2(t)dt$
5.	$OF = \mu(ITSE) + ZLG$
6.	$ZLG = (1-e^{-\beta}) * (OS + E_{ss}) + e^{-\beta}(t_s - t_r)$

simulation and optimization for a 2 MVA/400 V synchronous generator powered by a 3-phase diesel engine that features a mechanical coupling and an exciter system. Further integration with renewable energy sources can be investigated thanks to this investigation.

To achieve this goal, the following tasks must be completed:
1- determining the dynamic response of field voltage (V_f) and current (I_f) in the excitation system once there is a change in its load. It takes 3 techniques (PID, NN, and SA) for the best response.
2- must examine the exciter system's 3-phase voltage and current measurements over a 10-second time frame in order to confirm the built synchronous machine's functionality.

A. Literature Review

In both traditional and modern Electric Energy Systems (EES), Synchronous Generators (SGs) play a crucial role as voltage-regulating devices [12]. Currently, AVRs [13], or excitation systems [14], are used in microprocessor technology to achieve voltage regulation.

AVR systems have many non-linear components, which makes their modeling, design, work analysis, and testing extremely complex [10, 15–19]. Because of this, every component of the AVR design is typically approximated and described using basic transfer functions found in [16, 20–24]. All components, with the exception of the controller, are denoted by transfer functions of the first order [1, 3, 7, 19, 25–29]. On the other hand, some research also demonstrates that a third-order system represents the generator for AVR cycles [9]. The third-order model adds complexity to the system analysis. Conversely, it recognizes a more precise machine model. Additionally, generator models offered by fuzzy logic, neural networks, and similar techniques are used in several articles [9, 30].

According to the literature, using meta-heuristic algorithms like the Future Search Algorithm (FSA) [17] , the Hybrid Evolutionary Algorithm (HEA) [25], the Whale Optimization Algorithm (WOA) [20], the Chaotic Yellow Saddle Goatfish Algorithm (CYSGA) [16], the Local Unimodal sampling algorithm (LUSA) [26], Taguchi combined Genetic Algorithm

(TCGA) [31], the Particle Swarm Optimization (PSO) [3], the Simplified PSO (SPSO) [7], and the CRaziness based PSO (CRPSO) [28], Artificial Bee Colony (ABC) [28], The Chaotic Multi-Objective Optimization (CMOO) [32], Enhanced Crow Search Algorithm (ECSA) [18], Symbiotic Organisms Search Algorithm (SOSA) [33], Ant Colony Optimization (ACO) [21], Invasive Weed Optimization (IWO) [34], Sine Cosine Algorithm (SCA) [35], Differential Evolution (DE) [28], Chaotic Ant Swarm (CAS) [22], Equilibrium Optimizer Algorithm (EOA) [29], and Imperialist Competitive Algorithm (ICA) [36], It should be mentioned that determining the regulator's parameters is a significant issue that has been covered in a number of publications. A specific abbreviation appears in Table II.

II. THE PURPOSE AND GOALS OF THE RESEARCH

This research aims to contribute to more robust and efficient excitation control systems, enhancing the performance and stability of modern electric power systems by:

1. Analyze the dynamic response of field voltage and field current under varying loads.
2. Evaluate the effectiveness of PID, NN, and SA controllers with ISE objective function in optimizing voltage response.
3. Conduct a comparative analysis of the proposed controller techniques towards excitation system management. This could focus on enhancements in performance metrics, which include response time, stability, and disturbance rejection.

III. SYNCHRONOUS GENERATOR WITH EXCITATION SYSTEM

Synchronous generator is commonly used in an engine that produces electricity. In stator coils, a rotating magnetic field (typically generated by a DC magnet) generates electricity. This magnet can be powered externally, but it is more appropriate for placing the exciter, the small generator, on a single shaft inside the same container. To feed this magnet in any case, DC needs to be supplied to the rotor. A simple fix is two slip rings [37], but they need to be worn and cared for regularly. Any slipping contacts via the spinning rectifier are prevented by integrating a tiny AC generator as an exciter on the shaft of the rotor, rectified the current, and delivering it to the rotor coils all on the same shaft. The exciter gets its field current from a current that is sent into the exciter stator via the power output of the main generator.

This approach makes it possible to design a complex system with a simple yet efficient voltage control. In order to compensate for the primary generator's voltage drop as the load grows, the excitation must be increased. This means that the exciter must produce a higher field current, which can be achieved by increasing its excitation. Consequently, the main generator's voltage can be modified by utilizing the DC supply of the exciter stator. This regulation is carried out electrically by an automatic voltage regulator [38]. The controller controls the field current to keep the voltage output consistent across all load types, with a predetermined output voltage defined. Current brushless machines and synchronous generators have an AVR. Because of its residual magnetism, the machine may start itself. When it rotates, a tiny output voltage is created, and this voltage is then increased by a small current passing through the AVR and into the exciter [39]. This control loop generates the nominal output voltage among certain machine types. It's possible that the magnetism has disappeared.

A small synchronous machine attached to the main synchronous generator by a similar shaft provides the excitation method for large alternators. To accomplish current rectification and eliminate the need for slip rings to give DC power to the synchronous alternators' field, a revolving bridge diode is mounted on the shaft of a synchronous machine. Using speed as the mechanical input for the exciter machine, the synchronous generator and exciter are mechanically coupled [40]. Fig.2 depicts the synchronous generator with the exciter system, and Fig. 3 shows the excitation control techniques diagram .

The DC from the excitation system is crucial to the synchronous generator's producing stability because it maintains the magnetic connection between the rotor and stator windings. On the other hand, a generator's loss of excitation weakens the connection between the stator and rotor, leading to imbalances in mechanical and electrical power as well as faster rotor speeds than synchronous. Furthermore, if early protection fails to activate in the event of an excitation loss-relay, the generator and the grid could be destroyed.

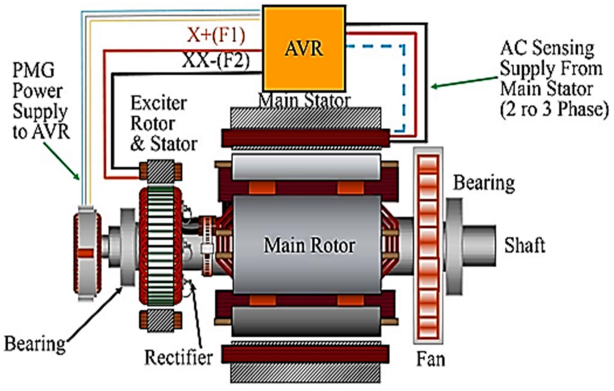

Fig. 2. Exciter setup with synchronous generator [41].

TABLE II.
DIFFERENT CONTROLLER WITH OPTIMIZATION ALGORITHM AND THE CORRESPONDING OBJECTIVE VALUE

NO.	Types		
	Controller	Proposed algorithm	Objective function
[10]	4 different PID	SA-MRF	ZLG
[15]	N/A	SA-EA	multiobjective
[16]	Fractional order PID (FOPID)	YSGA	OF
[17]	PID	FSA	ZLG
[18]	PID	ECSA	IAE
[19]	Robust model predictive (MPC)	AOA	ZLG
[20]	PID,PIDA	WOA	ISE
[21]	PID	ACO-NM	ZLG
[22]	FOPID	CAS	ISE
[23]	FOPID	CSA	ITSE
[24]	Sugeno fuzzy logic (SFL)	PSO	MF
[25]	PID	GA-PSO	ZLG
[26]	PID	LUS	ITSE
[27]	PID	ChO	ISE,IAE,ITSE,ITAE
[1]	PID	ABC,DE	ISE
[28]	PID	EO	ZLG
[29]	PID	PSO	Multi objective
[31]	PID	TCG	Multi objective
[32]	FOPID	CMOO	ITSE
[33]	PID	SOS	ITAE
[34]	FPID	IWO	ISE,IAE,ITSE,ITAE
[35]	FOPID	SCA	ZLG
[36]	gray PID (GPID)	IC	ZLG

As shown in Fig.3, the four fundamental excitation procedures. An AVR is used in all methods to provide DC output to the exciter stator. Every technique has a certain emphasis point.
• Shunt Method, also known as Self-Excited Excitation System: This technique gets the excitation current from the generator's stator. Practical and useful, it might not be appropriate for applications involving non-direct loads.
• Excited Excitation Boost System (EBS): This technique increases the excitation current by adding a second excitation source. Although it involves more wiring and elements, it is more effective.
• Permanent Magnet Generator (PMG): In this technique, the excitation current is produced by a permanent magnet. It is frequently utilized in situations where non-direct load operation is necessary.
• Auxiliary Winding (AUX): This technique provides the excitation current by means of an extra winding in the stator. Larger establishments find it more functional, although more parts and wiring are needed [41].

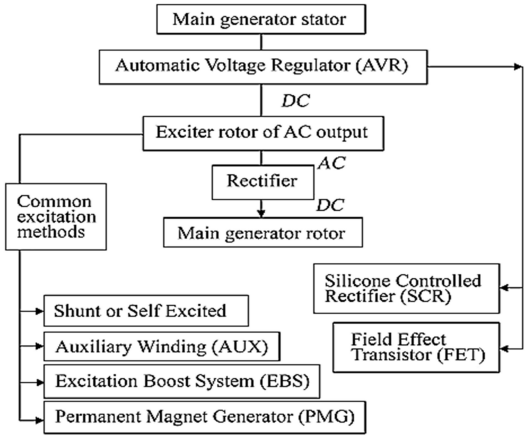

Fig. 3. Excitation control techniques [42].

A. AVR Controller Types

For any modern AVR to operate, the input reference voltage and output voltage must be compared. The difference is amplified using an amplifier, and then the amplified difference is utilized to control the regulatory element to minimize the voltage error. This creates a negative feedback control loop [43]. For getting stable output voltage there are many controllers adequate with this purpose.

1) The PID Controller

The proportional-integral-derivative (PID) controller method used to control the S.G.'s terminal voltage when it comes to varying operational loads and power factors. The operational principle involves detecting the terminal phase voltage and utilizing it as a feedback signal through the PID controller to generate a command-setting signal that adjusts the excitation voltage of the synchronous generator. However, publications also take into consideration an actual PID controller, which has a variable corresponding to the filter coefficient (marked as N) in addition to the preceding gains, as the ideal PID is impractical to implement [10]. For discrete input values, use the discrete formula of the PID controller (see Fig.4) for a discrete PID block diagram.

$$IdealPID \qquad C(S) = K_P + Ki/s + K_d.s \tag{1}$$

$$RealPID \quad C(S) = K_p + K_i/s + K_d \frac{N}{(1+N/s)} \tag{2}$$

$$DiscretePID\, C(S) = K_p + K_i \frac{T_S}{(z-1)} + K_d \frac{N}{(1+N.T_S/(Z-1))} \tag{3}$$

It hinges on the precise tuning of three key parameters in alignment with the system dynamics. When it comes to a proportional controller (K_p), its primary impact lies in diminishing the rise time while concurrently diminishing, albeit not completely eradicating, the steady-state error. Though it could worsen the transient response, an integral control (K_i) will have the impact of removing the steady-state inaccuracy. Enhancing the transient response, decreasing overshoot, and raising system stability are the outcomes of implementing a derivative control (K_d) [44]. Fig.5 shows AVR system with PID controller with consider the values of $K_p = 5, K_i = 8, K_d = 1$, and N = 100.

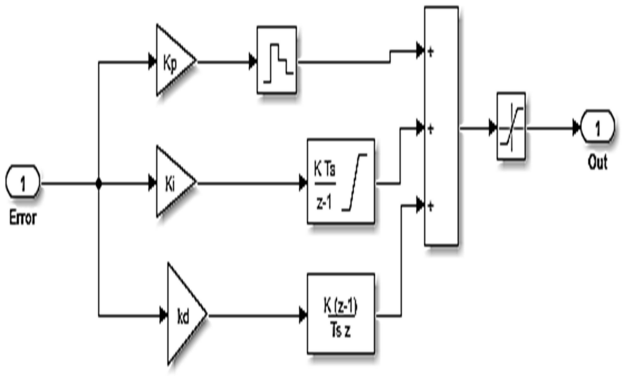

Fig. 4. Discrete PID block diagram

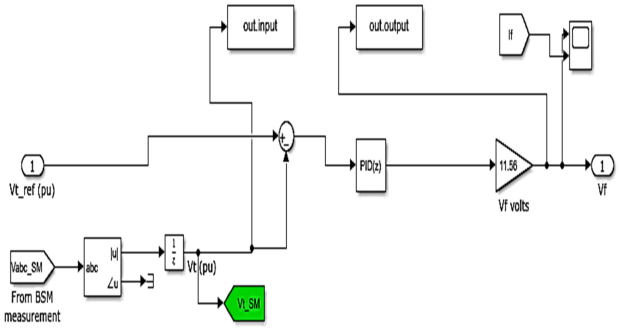

Fig. 5. AVR system with PID controller.

2) Neural Network Controller

The use of neural network-based techniques for the control of systems with complicated, linear, or non-linear dynamics has grown in prominence within the scientific literature. More specifically, adaptive designs, optimum control systems, and multivariable analysis are areas where a great deal of current knowledge exists, but neural reasoning-based approaches are still relatively new.

The synchronous generator control challenge is one example of a system with complex linear or non-linear dynamics for which current advancements in the field of neural networks (NN) may lead to novel strategy development. Recent years have seen a significant amount of study on the use of NN in dynamic systems control; notable works on this topic include those by Narendra et al. [45], Psaltis et al. [46]. Developing a neural network-based controller in the area of power system

controls through offline and/or online learning processes is the goal in order to get the responses that are required.
In this work, MATLAB's nnstart command was employed, which offers a strong tool for creating and refining AVRs for synchronous generators. Neural networks can be trained to manage the excitation system's field voltage by users using the Neural Network Fitting App and setting the network design.
According to Fig.6, the block architecture of the neural network training displays the schematic representation of a neuron on the left. A neuron typically receives multiple inputs. The elements in the input vector n=[n_1, n_2, n_j] are weighted by elements w_1, w_2, w_j of the weight matrix W respectively. The weighted inputs and the bias b of the neuron are added to create the net, this can be written as:

$$net = \sum_{j=1}^{R} n_j w_j + b \tag{4}$$

Subsequently, an active function f receives the net input n and produces the neuron output a:

$$a = f(net) \tag{5}$$

The log-sigmoid activation function is used in this investigation. The following expression can be used to describe it [47].

$$f(x) = 1/(1+e^{-x}) \tag{6}$$

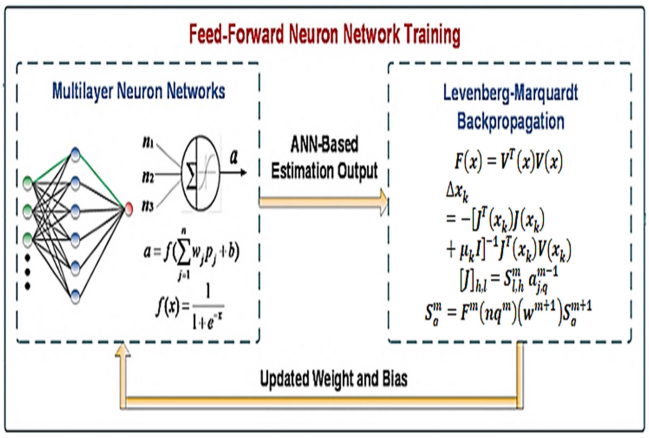

Fig. 6. Feed-forward neuron network training [47].

To train the neural network, the Levenberg-Marquardt method was employed. It is a common training technique. A function represented as the sum of squares of nonlinear functions is found to have a local minimum. The Levenberg-Marquardt approach combines the best features of both the steepest descent method and the Gauss-Newton algorithm, which are stability and speed, respectively [47].
Weight and bias tuning, as well as the inclusion of hidden layers and the choice of activation functions, are all possible with this program as shown in Figs. 7 and 8. This strategy can be especially useful for enhancing the power system's transient response and stability by adjusting to fluctuating loads and disturbances.

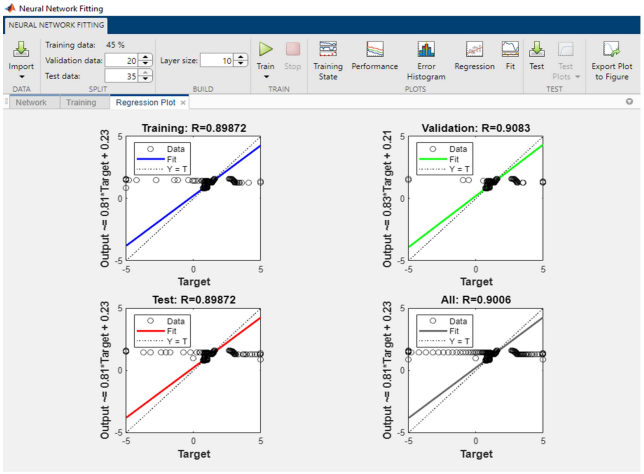

Fig. 7. Neural network fitting with 10 layers and 45 training data.

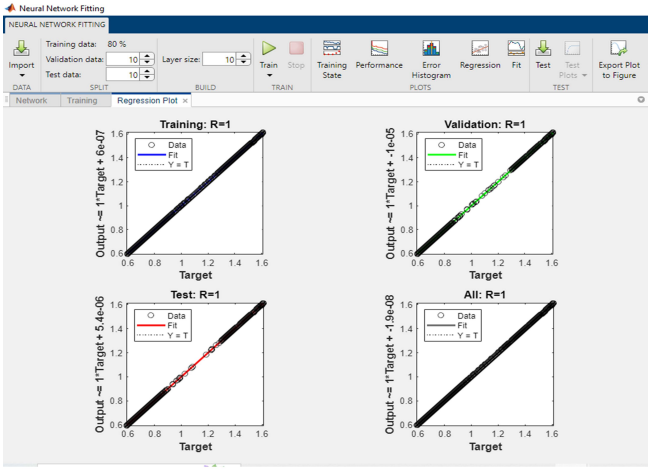

Fig. 8. Neural network fitting with 10 layers and 80 training data

Plots for several data sets (training, validation, test, and all data) illustrate the relationship between the target values and the network's output values. Each plot's R-value, or correlation coefficient, indicates how strong the linear link is; values

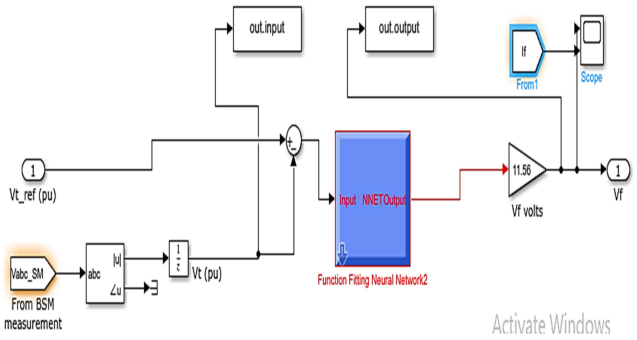

Fig. 9. AVR system with NN controller.

nearer 1 signify a stronger correlation. According to Fig.9, the network has undergone successful training and is capable of generalizing to voltage regulator.

3) *Simulated Annealing Controller*

Large-scale optimization issues can be solved using the technique known as simulated annealing (SA), which was initially presented by Kirkpatrik et al. [48]. The concept behind the process is similar to how molten metal cools and anneals. The system finds the least energy state for a cooling process that proceeds slowly. To make sure that a low energy state is reached, slow cooling is necessary.

By exiting local minima early in the computation, this research aims to avoid them. It just looks for the bottom of the local minimum toward the end of the calculation, when the temperature or likelihood of accepting a worse answer is almost zero. By reducing the cooling schedule, one can trade calculation time for a better probability of obtaining an accurate solution. The likelihood of identifying the ideal solution increases with slower cooling, but run times also increase. Therefore, the key to using this technique effectively is figuring out a cooling schedule that produces satisfactory results quickly. The first step in a typical SA process is to randomly generate an initial solution. The existing answer undergoes a modest, random modification in the beginning. Next, the objective function values of the new and existing solutions are computed and compared. If the new solution has a higher value or if SA implements the probability function, the old solution is replaced. Since temperature parameter T has the same significance as temperature during the physical annealing process, it is used in the calculation of this likelihood. The following conventional SA algorithm pseudo-code

Let T_0 = starting temperature , Iter = number of iterations, k is the time index of annealing set $T = T_0$
Let x =A random solution
Repeat:
For i = 0 to Iter 1
Let $f(x) = fitness\ of\ x$
Make a small change to x to make x_n
Let $f_n(x_n) = fitness\ \ of\ new\ point$
Calculate $\Delta f = f_n(x_n) - f(x)$
If $\Delta f \leq 0$ then
$x = x_n$
Else
If rand [0, 1] $< \exp\left(-\frac{\Delta f}{T}\right)$
$x = x_n$
End if
$T_{i+1} = T_0 \exp\big((c-1)k\big); \qquad 0 < c < 1$
End for
Output : the solution x.

Fig. 10. SA algorithm pseudo-code [49].

has been applied to our issue, see Fig.10. The initial temperature values, the cooling schedule, the number of cycles to be completed at each temperature, and the stopping condition to end the procedure make up the annealing program of the SA algorithm [49].

By definition, the majority of the characteristics in simulated annealing are fixed. The temperature is the only parameter that changes during the computation. Using the Boltzmann algorithm, an exponential schedule form, and the molting metals way, the system at higher temperatures and then gradually reduce it by a factor during the annealing process [49]:

$$T_{i+1} = T_0\ exp^{((C-1)K)} \tag{7}$$

where c is decided to be 0.8; and T_0, the starting temperature, is set to be approximately 1000; K is the time index of annealing that is calculated as the time step size multiplied by the i_{th} number of iteration and the total number of iterations is determined to be 100 for about 10s simulation. In this work, the integral squared error ISE of V_t of the SG is taken as the objective function (i.e., the goal of the minimization). The SA Simulink model, which is displayed in Fig.11, provides proof of the resilience and strength of SA in handling issues brought on by outside disruptions.

B. *Simulink Power Generator Model*

The synchronous generator's field terminals are directly linked to the rectifier bridge's output. It is not necessary to filter due to the large field inductance. Table III provides

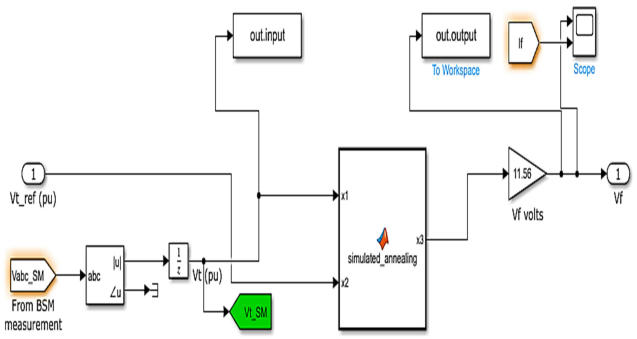

Fig. 11. AVR system with SA controller.

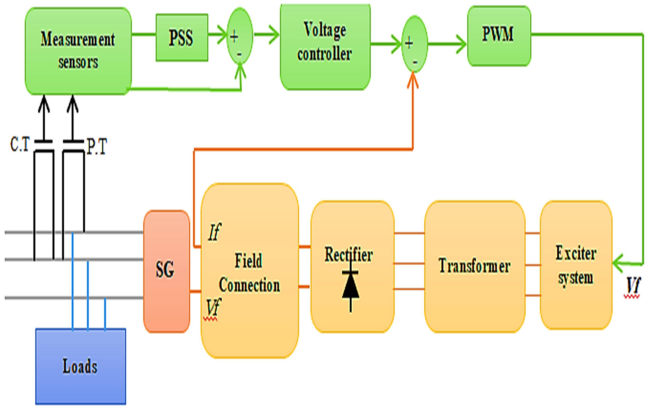

Fig. 12. Synchronous machine with exciter system and mechanical coupling

an explanation of the system's interesting content, and Fig.12 shows Simulink model under discussion in this work. MATLAB 2021 is used to implement the simulation.
Connecting the input V_f to the synchronous generator's real field terminals is crucial. The subsystem known as Field Connections measures the synchronous machine's field terminal voltage. It uses a current supply that is proportionate to the DC field current and powered by the bridge's DC current output. The field voltage that needs to be applied to the synchronous machine's inputs; it is equal to the voltage that exists across this current source. Controlling the exciter's field voltage allows to alter the generator's voltage.
The diesel engine provides all of the mechanical power for the main synchronous and the exciter machine. With a nominal field current I_{fn} of 100 A, the real voltage applied to the rotor (rather than the field voltage observed from the stator) can be used.

The synchronous machine is configured to deliver 500 kW, or 25 percentage of the rated value, in the interval of 0-3 seconds. A circuit breaker is used at $t = 3$ seconds to switch on an extra 1 MW.

IV. Result and Discussion

The results obtained for optimizing AVR controller. namely, we considered three regulators: PID, ANN, and SA algorithm.

A. Dynamic Reaction of the Field Voltage and Current When the Synchronous Generator Provides Power with An Interval Alter

When the power given by the SG changes, the excitation current increases to 105 A from 63 A at t = 3 seconds in order to keep the terminal voltage at 1 pu but V_t stabilize on the value of 0.42 instead of 1 without a controller. There is a high field inductance value, the voltage of the field V_f (as seen in Fig. 13 contains a ripple of 300 Hz that is hidden from view with the field current. Fig. 13 shows the response without a controller. On the left side of figures, the terminal voltage is shown in each case.

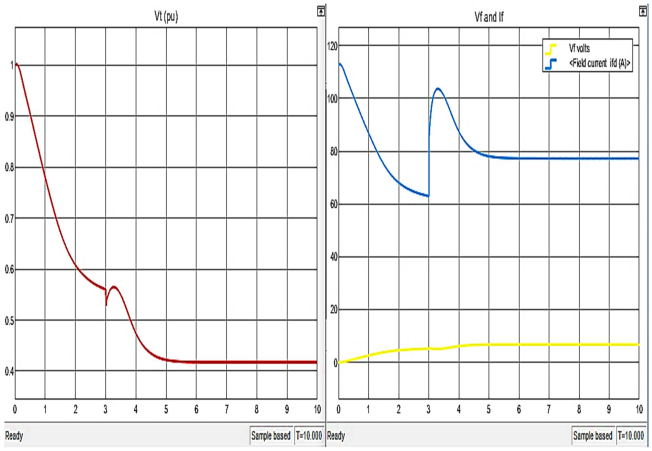

Fig. 13. Shows the synchronous machine's terminal voltage (pu), the field voltage (V) and the field current (A) without the simulation's controller

The PID is inserted in the AVR Simulink diagram and run first. In this case, as shown in Fig. 14 the values of V_f and I_f calculate from the AVR output. The excitation current increases to 185 A from 115 A at $t = 3$ seconds in order to keep the terminal voltage at 1 pu at $t = 7$ seconds.
It may design and enhance AVR controllers that ensure SGs

TABLE III.
LIST OF MATERIALS

Function	Essential component	Type
Main power generator	Synchronous	2 MVA, 400 V, 1.500 r.p.m,50 Hz
Exciter system	Small synchronous machine	8.1 MVA, 400 V, 1.500 r.p.m,50 Hz
Rectifier can receive the exciter's 400 V output voltage	Transformer	10 kVA , 400 V/ 12 V

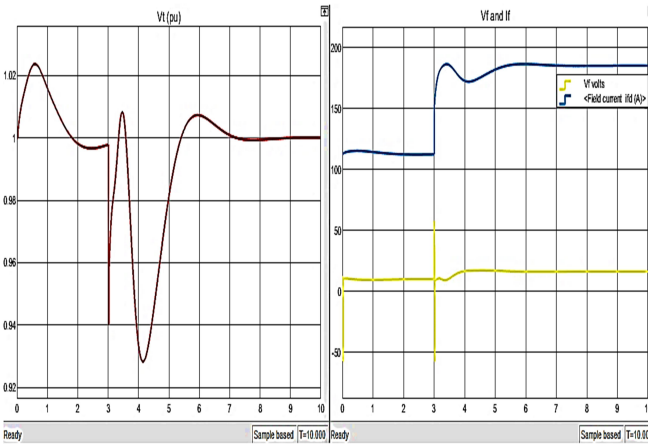

Fig. 14. Shows the synchronous machine's terminal voltage (pu), the field voltage (V) and the field current (A) with PID ,the simulation's controller.

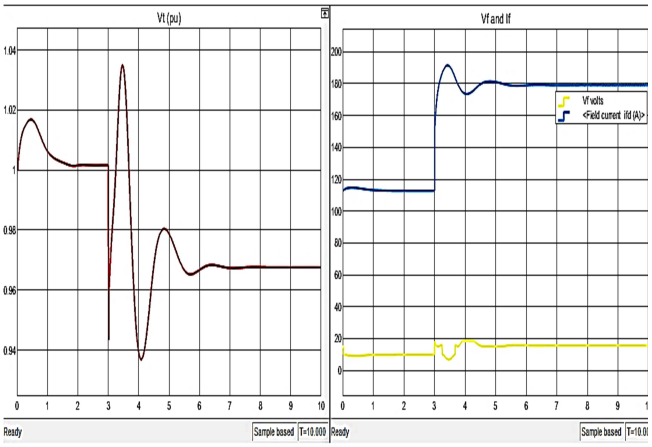

Fig. 15. Shows the synchronous machine's terminal voltage (pu), the field voltage (V) and the field current (A) with ANN ,the simulation's controller.

run dependably and effectively in a variety of power system configurations by using the flexibility of MATLAB and the capabilities of nnstart.The simulation results obtained with the neural network customized learning method are displayed in the Fig. 15. Setting up an appropriate network architecture is the initial stage in creating a NN controller.
There were no set protocols or standards in place before for choosing this structure. The process involves training the neural network with a limited number of neurons and observing the performance that results. If the performance is deemed insufficiently exact, the NN is trained again with a greater number of neurons and its accuracy is evaluated.We placed it into practice by using Matlab's nnstart function.It is simple to use; to provide the optimal response for field voltage and current, just match the target values with the network's output values. the excitation current increases to 190 A from 115 A at $t = 3$ seconds in order to keep the terminal voltage at 1 pu at $t = 6$ seconds.

We discovered that SA functions satisfactorily. After the first two seconds of operation, as seen in Fig. 16, the controller's effect becomes noticeable. It displays the SG system variable deviations' time response following the introduction of a disturbance.This shows how resilient and successful SA is at handling issues brought on by outside disruptions. the excitation current increases to 210 A from 115 A at $t = 3$ seconds in order to keep the terminal voltage at 1 pu. We can increase the accuracy by giving a high iteration, so we get the best result, but at long-term responses.

B. Monitoring the exciter system's 3-phase voltage and current readings over a 10-second time frame

In Figures (17, 18, and 19) the 3-phase voltage and current of the 2MVA/400V synchronous generator are displayed over a 10-second operation with a zoom region of change in power delivered by the SG for each case. As seen in Figures (17, 18, and 19) the synchronous machine's terminal voltage indicates that, upon load exchange during the 3-second transient, the

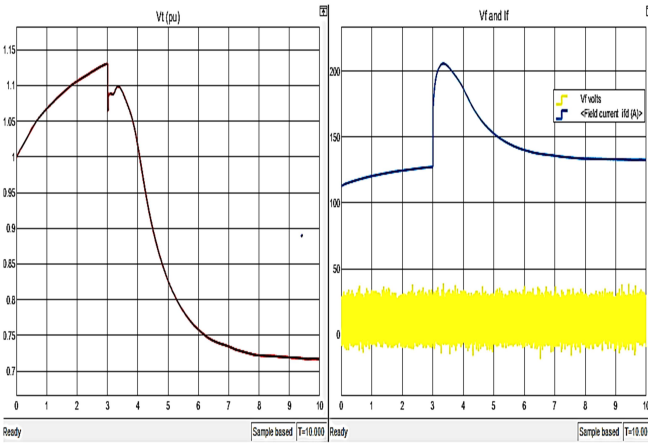

Fig. 16. Shows the synchronous machine's terminal voltage (pu), the field voltage (V) and the field current (A) with SA algorithm, the simulation's controller.

machine returns to its nominal voltage. The speed instruction maintains the nominal voltage of the output frequency of 50 Hz and an output speed equal to one pu. When evaluating the voltage and current waveforms under these variations, as demonstrated in Figures, the simulation complied with the findings and was reasonable. The PID and ANN offer exceptional replies in comparison to the SA algorithm, which produces the weakest response in terms of terminal voltage. This system with mechanical coupling is more viable for high-scale generation control because the suggested mechanical coupling with exciter for SGs offers greater resilience for managing the field current.

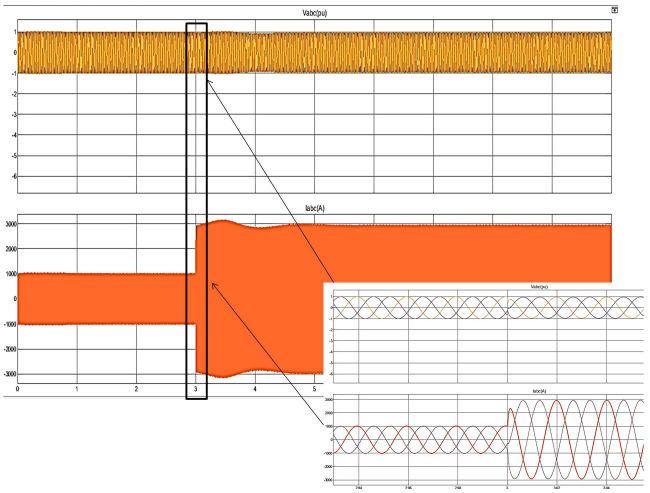

Fig. 17. Waveforms of the synchronous generator's three-phase voltage and current (2 MVA, 400V) with PID.

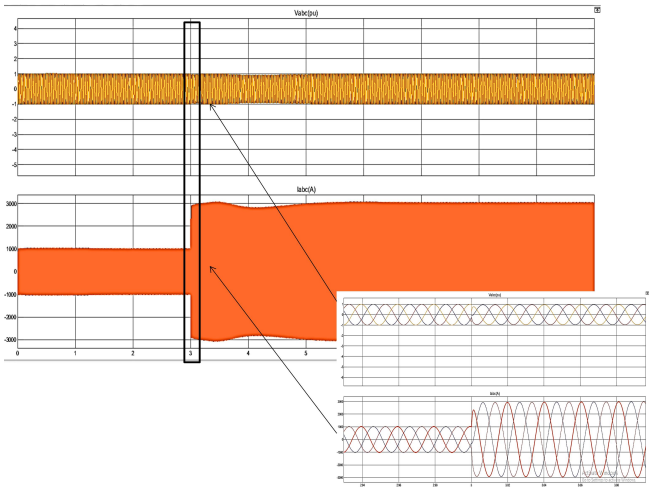

Fig. 18. Waveforms of the synchronous generator's three-phase voltage and current (2 MVA, 400V) with ANN.

V. CONCLUSION

This paper shows simulations to solve the SG control problem utilizing PID, ANN, and SA algorithms. Once second loads are connected through a circuit breaker, the controllers have been successfully utilized to build a control law that reduces oscillations within synchronous generators. According to the findings, PID and ANN controllers' responses stay the same across simulation, but Vt in SA will be decrees amount to 0.72. In addition, the results of our study have indicated that PID and neural controllers are potentially powerful methods; the results in both are similar in response, where stability of V_t begins after an interval of 3 to 7 sec. It had confirmed the robustness of the ANN when it possessed the capabilities necessary for finding the best solution for controlling the oscillations in synchronous generators. It was discovered that the SA controller worked to solve this issue. Compared to the NN controller, it is simpler to understand because it is intuitive and only requires a basic function of evaluations. In this instance, the data on terminal voltage demonstrate damped oscillations, but the system takes an interval of 3 to 8 seconds to reach its stable state at a 0.72 value of 1 pu. It would be beneficial to modify parallel computing algorithms to obtain real-time performances; nevertheless, this approach is left for later research. With some degree of confidence, it can be said that the controllers provide a workable solution for excitation control of SG issues in light of the simulation findings obtained.

CONFLICT OF INTEREST

The authors have no conflict of relevant interest to this article.

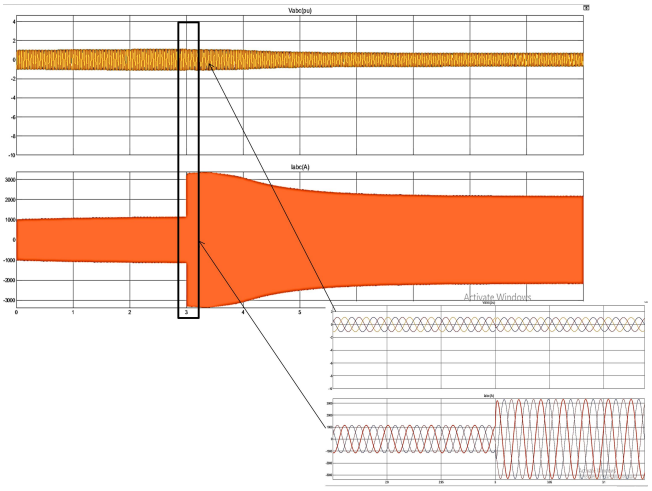

Fig. 19. Waveforms of the synchronous generator's three-phase voltage and current (2 MVA, 400V) with SA algorithm.

REFERENCES

[1] H. Gozde and M. C. Taplamacioglu, "Comparative performance analysis of artificial bee colony algorithm for automatic voltage regulator (avr) system," *Journal of the Franklin Institute*, vol. 348, no. 8, pp. 1927–1946, 2011.

[2] P. M. Anderson and A. A. Fouad, *Power system control and stability*. John Wiley & Sons, 2008.

[3] Z.-L. Gaing, "A particle swarm optimization approach for optimum design of pid controller in avr system," *IEEE transactions on energy conversion*, vol. 19, no. 2, pp. 384–391, 2004.

[4] J. L. Rodríguez-Amenedo and S. A. Gómez, "Damping low-frequency oscillations in power systems using grid-forming converters," *IEEE Access*, vol. 9, pp. 158984–158997, 2021.

[5] D. E. Rumelhart, J. L. McClelland, P. R. Group, *et al.*, *Parallel distributed processing, volume 1: Explorations in the microstructure of cognition: Foundations*. The MIT press, 1986.

[6] H. Bevrani, H. Golpîra, A. R. Messina, N. Hatziargyriou, F. Milano, and T. Ise, "Power system frequency control: An updated review of current solutions and new challenges," *Electric Power Systems Research*, vol. 194, p. 107114, 2021.

[7] S. Panda, B. K. Sahu, and P. K. Mohanty, "Design and performance analysis of pid controller for an automatic voltage regulator system using simplified particle swarm optimization," *Journal of the Franklin Institute*, vol. 349, no. 8, pp. 2609–2625, 2012.

[8] Z. Dongli, T. Yinggan, and G. Xinping, "Optimum design of fractional order pid controller for an avr system using an improved artificial bee colony algorithm [j]," *Acta Automatica Sinica*, vol. 40, no. 5, pp. 973–980, 2014.

[9] M. Zamani, M. Karimi-Ghartemani, N. Sadati, and M. Parniani, "Design of a fractional order pid controller for an avr using particle swarm optimization," *Control Engineering Practice*, vol. 17, no. 12, pp. 1380–1387, 2009.

[10] M. Micev, M. Ćalasan, Z. M. Ali, H. M. Hasanien, and S. H. A. Aleem, "Optimal design of automatic voltage regulation controller using hybrid simulated annealing–manta ray foraging optimization algorithm," *Ain Shams Engineering Journal*, vol. 12, no. 1, pp. 641–657, 2021.

[11] S. Ekinci and B. Hekimoğlu, "Improved kidney-inspired algorithm approach for tuning of pid controller in avr system," *IEEE Access*, vol. 7, pp. 39935–39947, 2019.

[12] T. A. Lipo, *Analysis of synchronous machines*. CRC press, 2017.

[13] A. Sikander and P. Thakur, "A new control design strategy for automatic voltage regulator in power system," *ISA transactions*, vol. 100, pp. 235–243, 2020.

[14] J. K. Nøland, S. Nuzzo, A. Tessarolo, and E. F. Alves, "Excitation system technologies for wound-field synchronous machines: Survey of solutions and evolving trends," *IEEE Access*, vol. 7, pp. 109699–109718, 2019.

[15] F. J. Rodriguez, C. Garcia-Martinez, and M. Lozano, "Hybrid metaheuristics based on evolutionary algorithms and simulated annealing: taxonomy, comparison, and synergy test," *IEEE Transactions on Evolutionary Computation*, vol. 16, no. 6, pp. 787–800, 2012.

[16] M. Micev, M. Ćalasan, and D. Oliva, "Fractional order pid controller design for an avr system using chaotic yellow saddle goatfish algorithm," *Mathematics*, vol. 8, no. 7, p. 1182, 2020.

[17] M. Elsisi and M. Soliman, "Optimal design of robust resilient automatic voltage regulators," *ISA transactions*, vol. 108, pp. 257–268, 2021.

[18] A. K. Bhullar, R. Kaur, and S. Sondhi, "Enhanced crow search algorithm for avr optimization," *Soft Computing*, vol. 24, no. 16, pp. 11957–11987, 2020.

[19] M. Elsisi, M.-Q. Tran, H. M. Hasanien, R. A. Turky, F. Albalawi, and S. S. Ghoneim, "Robust model predictive control paradigm for automatic voltage regulators against uncertainty based on optimization algorithms," *Mathematics*, vol. 9, no. 22, p. 2885, 2021.

[20] A. M. Mosaad, M. A. Attia, and A. Y. Abdelaziz, "Whale optimization algorithm to tune pid and pida controllers on avr system," *Ain Shams Engineering Journal*, vol. 10, no. 4, pp. 755–767, 2019.

[21] M.-J. Blondin, J. Sanchis, P. Sicard, and J. Herrero, "New optimal controller tuning method for an avr system using a simplified ant colony optimization with a new constrained nelder–mead algorithm," *Applied soft computing*, vol. 62, pp. 216–229, 2018.

[22] Y. Tang, M. Cui, C. Hua, L. Li, and Y. Yang, "Optimum design of fractional order piλdμ controller for avr system using chaotic ant swarm," *Expert Systems with Applications*, vol. 39, no. 8, pp. 6887–6896, 2012.

[23] A. Sikander, P. Thakur, R. C. Bansal, and S. Rajasekar, "A novel technique to design cuckoo search based fopid controller for avr in power systems," *Computers & Electrical Engineering*, vol. 70, pp. 261–274, 2018.

[24] V. Mukherjee and S. Ghoshal, "Intelligent particle swarm optimized fuzzy pid controller for avr system," *Electric Power Systems Research*, vol. 77, no. 12, pp. 1689–1698, 2007.

[25] C.-C. Wong, S.-A. Li, and H.-Y. Wang, "Hybrid evolutionary algorithm for pid controller design of avr system," *Journal of the Chinese institute of engineers*, vol. 32, no. 2, pp. 251–264, 2009.

[26] P. K. Mohanty, B. K. Sahu, and S. Panda, "Tuning and assessment of proportional–integral–derivative controller for an automatic voltage regulator system employing local unimodal sampling algorithm," *Electric Power Components and Systems*, vol. 42, no. 9, pp. 959–969, 2014.

[27] L. dos Santos Coelho, "Tuning of pid controller for an automatic regulator voltage system using chaotic optimization approach," *Chaos, Solitons & Fractals*, vol. 39, no. 4, pp. 1504–1514, 2009.

[28] M. Micev, M. Ćalasan, and D. Oliva, "Design and robustness analysis of an automatic voltage regulator system controller by using equilibrium optimizer algorithm," *Computers & Electrical Engineering*, vol. 89, p. 106930, 2021.

[29] M. A. Sahib and B. S. Ahmed, "A new multiobjective performance criterion used in pid tuning optimization algorithms," *Journal of advanced research*, vol. 7, no. 1, pp. 125–134, 2016.

[30] D. Gillard and K. Bollinger, "Neural network identification of power system transfer functions," *IEEE transactions on energy conversion*, vol. 11, no. 1, pp. 104–110, 1996.

[31] H. M. Hasanien, "Design optimization of pid controller in automatic voltage regulator system using taguchi combined genetic algorithm method," *IEEE systems journal*, vol. 7, no. 4, pp. 825–831, 2012.

[32] I. Pan and S. Das, "Frequency domain design of fractional order pid controller for avr system using chaotic multi-objective optimization," *International Journal of Electrical Power & Energy Systems*, vol. 51, pp. 106–118, 2013.

[33] E. Çelik and R. Durgut, "Performance enhancement of automatic voltage regulator by modified cost function and symbiotic organisms search algorithm," *Engineering science and technology, an international journal*, vol. 21, no. 5, pp. 1104–1111, 2018.

[34] N. Alawad and N. Rahman, "Tuning fpid controller for an avr system using invasive weed optimization algorithm," *Jordan J. Electr. Eng*, vol. 6, no. 1, p. 1, 2020.

[35] M. S. Ayas and E. Sahin, "Fopid controller with fractional filter for an automatic voltage regulator," *Computers & Electrical Engineering*, vol. 90, p. 106895, 2021.

[36] Y. Tang, L. Zhao, Z. Han, X. Bi, and X. Guan, "Optimal gray pid controller design for automatic voltage regulator system via imperialist competitive algorithm," *International Journal of Machine Learning and Cybernetics*, vol. 7, pp. 229–240, 2016.

[37] H. Gorginpour, "Optimal design of brushless ac exciter for large synchronous generators considering grid codes requirements," *IET Generation, Transmission & Distribution*, vol. 12, no. 17, pp. 3954–3962, 2018.

[38] E. Abramov, T. Vekslender, O. Kirshenboim, and M. M. Peretz, "Fully integrated digital average current-mode control voltage regulator module ic," *IEEE journal of emerging and selected topics in power electronics*, vol. 6, no. 2, pp. 485–499, 2017.

[39] W. Liu, G. Qin, Q. Zhu, and G. Hu, "Synchronous extraction circuit with self-adaptive peak-detection mechanical

switches design for piezoelectric energy harvesting," *Applied Energy*, vol. 230, pp. 1292–1303, 2018.

[40] "Generator excitation control systems and methods," *Available at: https://www.generatorsource.com/Generator-ExcitationMethods.aspx*.

[41] "Generator excitation control systems and methods - mid-america engine," *Available at: https://www.midamericaengine.com/generator-excitation-control-systems-methods/*.

[42] R. L. Damij, "Development of mechanical coupling and exciter system in synchronous generators," *Eastern-European Journal of Enterprise Technologies*, vol. 6, no. 8, p. 114, 2021.

[43] R. S. Lodhi and A. Saraf, "Survey on pid controller based automatic voltage regulator," *International Journal of Advanced Research in Electrical, Electronics and Instrumentation Engineering*, vol. 5, no. 9, pp. 7424–7429, 2016.

[44] S. Yu and X. Li, "Proportional–integral–derivative controller performance assessment and retuning based on general process response data," *ACS omega*, vol. 6, no. 15, pp. 10207–10223, 2021.

[45] K. Narendra, "Identification and control of dynamical systems using neural networks," *IEEE Transactions on Neural Networks*, vol. 1, no. 1, pp. 183–192, 1989.

[46] M. Saerens and A. Soquet, "A neural controller," in *1989 First IEE International Conference on Artificial Neural Networks,(Conf. Publ. No. 313)*, pp. 211–215, IET, 1989.

[47] C. Lv, Y. Xing, J. Zhang, X. Na, Y. Li, T. Liu, D. Cao, and F.-Y. Wang, "Levenberg–marquardt backpropagation training of multilayer neural networks for state estimation of a safety-critical cyber-physical system," *IEEE Transactions on Industrial Informatics*, vol. 14, no. 8, pp. 3436–3446, 2017.

[48] S. Kirkpatrik, "Optimization by simulated annealing," *IBM Thomas J. Watson Research Center Report*, 1982.

[49] A. Al-Dmour, "Excitation control of a synchronous generator using neural networks and simulated annealing controllers," *Jordan Journal of Electrical Engineering*, vol. 2, no. 3, pp. 253–269, 2016.